Optics Communications ■ (■■■■) ■■■–■■■

Contents lists available at ScienceDirect

Optics Communications

journal homepage: www.elsevier.com/locate/optcom

Broadband mid-IR supercontinuum generation in As_2Se_3 based chalcogenide photonic crystal fiber: A new design and analysis

Than Singh Saini, Ajeet Kumar, Ravindra Kumar Sinha *

TIFAC-Center of Relevance and Excellence in Fiber Optics and Optical Communication, Department of Applied Physics, Delhi Technological University, Delhi 110042, India

ARTICLE INFO

Article history:
Received 20 December 2014
Received in revised form
21 February 2015
Accepted 24 February 2015

Keywords:
Highly nonlinear photonic crystal fiber
All-normal dispersion fiber
Supercontinuum generation

ABSTRACT

A new design of a triangular-core photonic crystal fiber in As_2Se_3-based chalcogenide glass with all-normal, nearly zero flat-top dispersion has been proposed for supercontinuum generation. Simulated results indicate that ultra-broadband supercontinuum spanning 1.9–10 μm can be obtained using only 6 mm long PCF pumped with 50 femto-second laser pulses operated at 4.5 μm. In comparison to previously reported work we have obtained ultra-broadband supercontinuum spectra using relatively very low peak power of incident pulses. Proposed photonic crystal fiber structure is applicable in bio-molecular sensing and infrared spectroscopy.

1. Introduction

Photonic crystal fibers (PCFs) or holy fibers (HFs) are fascinating because of their unique linear and nonlinear properties such as dispersion management, high birefringence, large-mode-area with endlessly single-mode operation, high power delivery and supercontinuum generation (SCG) [1–10]. Supercontinuum (SC) is the nonlinear optical process where ultra-short pulse of laser light is evolved into the light with very broad spectral bandwidth. SCG is outcome of various nonlinear, such as self-phase modulation (SPM), cross-phase modulation (XPM), self-steepening, four-wave mixing (FWM), stimulated Raman scattering (SRS) and dispersion effects. SCG occurs when narrow-band input optical pulses undergo extreme nonlinear spectral broadening to yield spectrally continuous white light output while passing through optical fibers [1].

The applications of SC fall in different fields such as telecommunication, optical metrology, optical coherence tomography (OCT), nonlinear microscopy, cosmological studies, ultra-short pulse and frequency combs generation [11–17]. Initially, SCG in single-mode fiber was used around 1994 to obtain picosecond pulses of multiple wavelengths for wavelength division multiplexing (WDM) communication system [17]. The phenomenon of SCG was first time studied around 1970 in solid and gaseous nonlinear media by Alfano et al. [18], while supercontinuum in PCF is demonstrated by Ranka et al. in the year 2000 [19]. The progress of SCG in PCF has also been reported in several reviews [3–20,21].

In order to simulate SCG, an understanding of the media in which they are generated, is needed. PCFs in high-index non-silica glasses such as tellurite, bismuth, fluoride and chalcogenide have advantages over silica-based PCFs in various applications of highly nonlinear optical fibers and mid-infrared transmission [22–24]. Chalcogenide glasses are excellent candidates as some of its compositions have optical transparency up to 25 μm in mid-IR region [25]. In addition to broadband mid-IR transmission window, chalcogenide glasses possess very large linear and nonlinear refractive indices [26].

An experimental demonstration of SCG in the spectral range of 2.1 to 3.2 μm using hexagonal structure of As_2Se_3 chalcogenide PCF was presented by Shaw et al. [27]. Yeom et al. first time demonstrated the SCG in dispersion engineered As_2Se_3 fiber taper [28]. Hudson et al. reported experimentally the broadening of SC spectrum spanning 0.97–1.99 μm in a sulfide-based chalcogenide tapered fiber using very low pulse energy [29]. The basic elements of tapered chalcogenide optical fibers have been reviewed for supercontinuum generation [30]. Lamont et al. fabricated first time an anomalous dispersion engineered chalcogenide planar waveguide for supercontinuum genearation [31]. In the recent past, Hu et al. introduced a design procedure, which can be used to maximize the band-width of supercontinuum generation in As_2Se_3 chalcogenide PCFs, for more than 4 μm band-width of SC with input pulse at 2.5 μm [32]. A detailed comparison between the theoretical and experimental investigation of SCG in commercially available ZBLAN optical fibers have been presented in the Ref. [33].

* Corresponding author.
E-mail address: dr_rk_sinha@yahoo.com (R. Kumar Sinha).

http://dx.doi.org/10.1016/j.optcom.2015.02.049
0030-4018/

Kubat et al. presented a numerical design optimization of ZBLAN fibers for mid-IR SC sources with spectra covering 1 – 4.5 μm regime using direct pumping with 10 ps pulses from mode-locked Yb and Er lasers [34]. In Ref. [35], the authors have experimentally demonstrated the SCG covering 0.9 – 9 μm with the help of commercially available ZBLAN fiber and commercially available chalcogenide PCF. Hudson et al. demonstrated SC spectrum spanning 1.6–5.9 μm at −20 dB level in a step-index chalcogenide fiber using an optical parametric chirped pulse amplifier at 3.1 μm [36]. Numerical modeling of broadband mid-IR SCG spanning from 3 μm to 12.5 μm has been presented in a step-index fiber pumped at 4.5 μm with 0.75 KW pump power [37].

In above mentioned works, SC have been generated in fiber structures which offer group velocity dispersion (GVD) profile in both normal and anomalous dispersion regime. If the pump wavelength lies in anomalous dispersion regime, the flatness of SC is distorted due to soliton fission for pumping with femtosecond pulses. However, the probability of soliton fission can be completely removed by designing fiber with all-normal dispersion regime [38,39]. Thus, the phenomenon of SPM and optical wave breaking leads to SCG in the fiber having all-normal dispersion. This makes the SC with very low noise. Such broad-band SC is suitable for time-resolved applications. One of the possibilities for generating SC in the normal dispersion regime is to pump the fiber far below the zero dispersion wavelength (ZDW), so that the generated spectrum does not extend into the anomalous dispersion region. However, this would require high power or very short pulses to overcome the short effective interaction length due to high value of dispersion. For obtaining the intrinsic coherent property of super continuum generation, the PCFs with all-normal and flat-top dispersion are desirable. In this regard, various efforts have been done earlier to obtain all-normal flat-top dispersion in chalcogenide PCF [40–42].

SCG in all-normal dispersion PCF has been investigated numerically using high energy femtosecond pulses to obtain coherent octave spanning SC spectra [40]. A PCF design in chalcogenide glass has been presented with all-normal flat dispersion for applications in fiber lasers, pulse compression and multi-wavelength optical sources in the mid-infrared region [41]. Recently, a numerical simulation on the coherent time-critical SCG in As_2S_3-based chalcogenide microstructured fiber with all-normal flat-top dispersion profile has been carried out for 2–5 μm spectral range [42]. Mid-IR SC spectra spanning 1.795–6.525 μm has been achieved in 8 mm length of As_2Se_3 nanofiber with input pulse energy of 100 nJ [43]. Very recently, Klimczak et al. demonstrated first experimental report of all-normal dispersion SCG spanning over an octave from 900 nm to 2300 nm in all-solid soft glass PCF using 75 fs pulses centered at 1550 nm [44].

In this paper, we report a new design of triangular-core (TC) PCF and have used the same for ultra-broadband SCG in mid-IR region. We have also investigated the effects of input pulse parameters (such as: peak power and pulse width in terms of full width at half maxima) and propagation length of fiber on evolution of SCG in proposed TC PCF. It is important to mention here that our proposed TC PCF design is able to generate ultra-broadband mid-IR SC extending from 1.9 μm to 10 μm in only 6 mm long PCF with relatively much lower peak power of 700 W, in comparison to recently demonstrated broadband mid-IR SCG extending from 2 μm to 10 μm with peak power >5 kW at 4 μm in 6 cm long As_2Se_3 PCF [45].

A mid-IR pulsed laser operated at 4.5 μm based on praseodymium (Pr^{3+}) doped chalcogenide fiber has been considered for the formation of mid-IR SC [46]. A hyperbolic secant shaped pulse has been assumed with a temporal duration (T_{FWHM}) of 50 fs and peak power at 700 W for numerical simulation of SCG in the proposed TC PCF.

This paper is organized in five sections. Section 1 provides a brief introduction and overview of previous works on SCG in chalcogenide PCF. In Section 2, detailed description of method of analysis is given. Section 3 explains the designing of proposed TC PCF for all-normal, nearly zero flattened dispersion. Section 4 is devoted to the generation of ultra-broad band supercontinuum in proposed TC PCF. Finally, conclusions and applications of this work are summarized in Section 5.

2. Method of analysis

2.1. Linear characteristics of PCF structure

To simulate the effective index of fundamental mode propagating through proposed photonic crystal fiber, a full vectorial finite element method (FEM) based software 'COMSOL Multiphysics' has been employed. For calculating the wavelength dependent refractive index of material following Sellmeier equation has been used [41]

$$n(\lambda) = \sqrt{a + b/\lambda^2 + c/\lambda^4} \tag{1}$$

where a, b and c are coefficients. The values of coefficients are: $a=7.56$, $b=1.03\ \mu m^2$ and $c=0.12\ \mu m^4$ for As_2Se_3 based chalcogenide glass which we have used as a PCF material in this paper.

The group velocity dispersion plays an important role in SCG because it determines the extent to which different spectral components of an ultra-short pulse propagate at different phase velocities in the photonic crystal fiber. The group velocity dispersion $D(\lambda)$ is calculated from wavelength dependent effective indices of propagating mode by using the following formula

$$D(\lambda) = -\frac{\lambda}{c}\frac{d^2\mathrm{Re}(n_{eff})}{d\lambda^2} \tag{2}$$

where c is the velocity of light in free space, $\mathrm{Re}(n_{eff})$ is the real part of the effective index of mode. Both material and waveguide dispersion are included in the above equation as Sellmeier equation is taken into account while calculating n_{eff}.

The effective area of propagating mode in the PCF has been calculated using the following relation [1]

$$A_{eff} = \frac{\left(\iint_{-\infty}^{\infty} |E|^2 dx\, dy\right)^2}{\left(\iint_{-\infty}^{\infty} |E|^4 dx\, dy\right)} \tag{3}$$

2.2. Nonlinear characteristics of PCF structure

Nonlinearity in PCF is the most important parameter which must be studied more rigorously in order to get accurate results. The nonlinear coefficient γ, offered by PCF can be calculated by [1]

$$\gamma = \frac{2\pi n_2}{\lambda A_{eff}} \tag{4}$$

where, n_2 is the nonlinear refractive index of material (for As_2Se_3; $n_2 = 2.4\times10^{-17}\ m^2/W$ [47]), λ is the pump wavelength and A_{eff} is the effective area of fundamental mode. For broader supercontinuum generation (SCG) the nonlinear coefficient should be as high as possible. The value of γ can be enhanced by taking material with high nonlinear refractive index and/or by designing a PCF with smaller effective mode area.

To simulate SC, the following generalized nonlinear Schrodinger equation (GNLSE) has to be solved for output pulse envelope, $A(z, t)$ [1]

$$\frac{\partial A}{\partial z} + \frac{\alpha}{2}A - \left(\sum_{n\geq 2}\beta_n \frac{i^{n+1}}{n!}\frac{\partial^n A}{\partial t^n}\right) = i\gamma\left(1 + \frac{i}{\omega_o}\frac{\partial}{\partial t}\right)\left[A(z,t)\int_{-\infty}^{\infty} R(t')\,|A(z,t-t')|^2 dt' + i\Gamma_R(z,t)\right] \quad (5)$$

The left hand side of Eq. (5) deals with linear propagation effects while the right hand side of this deals with nonlinear effects of PCF structure. α represents the power loss in the PCF as the light travels through it. The typical value of simulated confinement loss is equal to 0.03 dB/mm at 4.5 μm wavelength. The propagation constant (β) at any frequency (ω), relative to pulse central frequency (ω_0), can be expanded as Taylor series expansion [3]

$$\beta(\omega) = \beta(\omega_0) + \beta_1(\omega_0)(\omega-\omega_0) + \frac{1}{2!}\beta_2(\omega_0)(\omega-\omega_0)^2 + \frac{1}{3!}\beta_2(\omega_0)(\omega-\omega_0)^3 + \ldots \quad (6)$$

where $\beta_n(\omega_0) = d^n\beta/d\omega^n$ first term in the right hand side of Eq. (6) gives the effective index of the propagating mode and the second and third terms are related to the group velocity and the group velocity dispersion (GVD) of the pulse respectively.

$R(t')$ is the nonlinear response function and takes account of the electronic and nuclear contributions and takes the form

$$R(t') = (1 - f_R)\delta(t' - t_e) + f_R\, h_R(t') \quad (7)$$

where, f_R is the fractional contribution of the Raman response to the total linear response. For As_2Se_3 chalcogenide glasses the fractional contribution $f_R = 0.115$ [47]. t_e is the instantaneous electronic contribution and $t_e = 1$ has been considered in the simulation. $h_R(t')$ is the Raman response function and contains information on the vibration of material molecules as light passes through the fiber.

The Raman response function $h_R(t')$ can be calculated by most common and approximate analytic form which is given by

$$h_R(t') = \frac{\tau_1^2 + \tau_2^2}{\tau_1\tau_2}\exp\left(-\frac{t'}{\tau_2}\right)\sin\left(\frac{t'}{\tau_1}\right) \quad (8)$$

where, Raman period $\tau_1 = 23.1$ fs and life time $\tau_2 = 195$ fs for As_2Se_3 based glasses [47].

The term Γ_R deals with the effect of spontaneous Raman noise. In our study, we consider the hyperbolic secant pulse which is expressed as

$$A(z=0,t) = \sqrt{P_0}\,\mathrm{sec}\,h\left(\frac{t}{t_o}\right) \quad (9)$$

where, t_0 is related to the pulse duration (i.e. full-width at half maximum (T_{FWHM})) as $t_0 = T_{FWHM}/1.7627$ and P_0 is the peak power of input pulse.

3. Design of proposed TC PCF

We present a new triangular-core photonic crystal fiber structure with four layers of air holes arranged in hexagonal pattern in As_2Se_3-based chalcogenide glass as shown in Fig. 1(a). Three air holes have been removed from the center to make triangular core of the PCF. The center to center distance of holes is taken as constant and represented by Λ. The diameter of air holes in first, third and fourth rings have been considered identical and defined by d_1, while the diameter of air holes in second ring is d_2, which is comparatively larger than d_1. To obtain the efficient SCG the structural parameters have been optimized for getting all-normal, near zero flat-top dispersion. Simulated electric field distribution of propagating mode in proposed TC PCF at 4.5 μm has been shown in Fig. 1(b).

In order to obtain efficient ultra-broad-band SC in proposed TC PCF, we have optimized the structural parameters (i.e. Λ, d_1 and d_2) for all-normal flat-top dispersion. For this purpose, initially we have simulated the effect of various values of pitch (Λ) on dispersion characteristic while keeping other parameters fixed (i.e. $d_1 = 420$ nm and $d_2 = 820$ nm) within the spectral range from 2.5 μm to 5.5 μm. This feature of structure has been shown in Fig. 2. It is to be noted that, at $\Lambda = 1$ μm the dispersion curve lies in both normal and anomalous dispersion regime and it start to shift towards normal dispersion regime on increasing the value of Λ. When $\Lambda = 1.2$ μm the dispersion curve lies in normal regime within the entire spectral range of 2.5–5.5 μm.

Now, influence of the hole diameter, d_1 (while keeping other parameters fixed; i.e. $\Lambda = 1.2$ μm and $d_2 = 820$ nm) on the dispersion characteristics of proposed structure has been illustrated in Fig. 3. It is clear from this figure that the dispersion characteristic does not change significantly on changing d_1. Therefore, it seems very difficult to get desire dispersion characteristic of structure using d_1. However, dispersion characteristic of structure can be tuned easily with air hole diameter d_2 in second ring of PCF structure. This feature of proposed structure has been illustrated in Fig. 4. The dispersion curve starts to shift toward the anomalous dispersion regime from normal dispersion regime on increasing d_2. It is to be noted that all-normal flat-top dispersion characteristic with dispersion value approximately − 2 ps/(nm km) within the spectral range from 4.4 μm to 4.8 μm can be achieved when $d_2 = 900$ nm. The above analysis and simulated results lead us to conclude that by careful choice of the structural parameter d_2 one can control and obtain the desired dispersion characteristic of

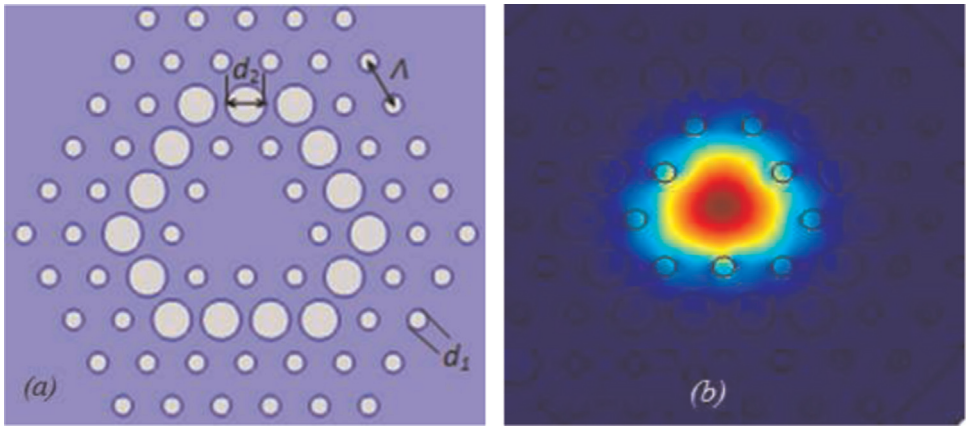

Fig. 1. (a) Transverse cross-section of proposed triangular-core PCF structure. (b) The electric field distribution of propagating mode at 4.5 μm.

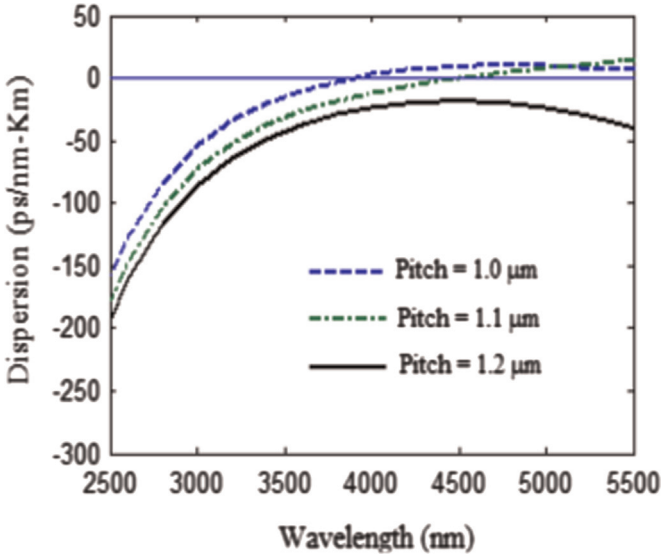

Fig. 2. Influence of the pitch (Λ) on dispersion characteristics of proposed structure while keeping other parameters fixed (i.e. d_1=420 nm and d_2=820 nm).

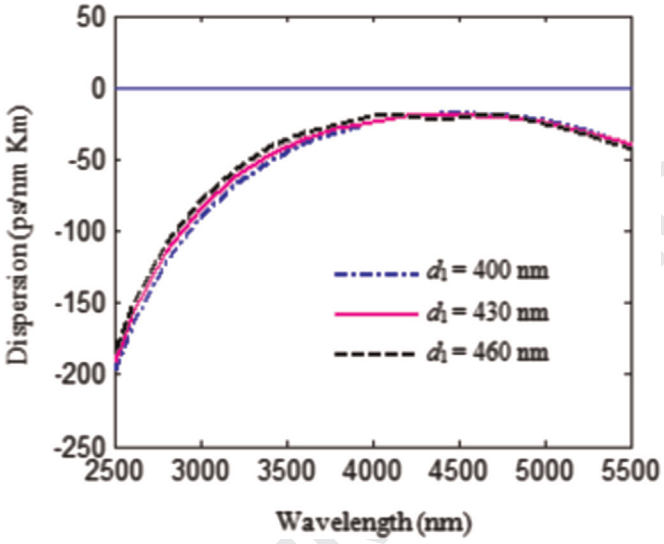

Fig. 3. Influence of the hole diameter (d_1) on dispersion characteristics of proposed structure while keeping other parameters fixed (i.e. Λ=1.2 μm and d_2=820 nm).

proposed TC PCF.

The confinement loss of propagating mode in the spectral range of 2–10 μm is shown in Fig. 5. At pump wavelength, (i.e. 4.5 μm) the structure offers 0.03 dB/mm loss for propagating mode.

For optimized geometrical parameters (as shown in Table 1), the wavelength dependent effective mode area of propagating mode and corresponding nonlinear coefficient have been illustrated in Fig. 6. Simulated results show that the proposed TC PCF structure offers nonlinear coefficient (γ) as high as 5449 W^{-1} km^{-1} with effective mode area of 6.15 μm^2 at 4.5 μm input pulse wavelength.

From the manufacturing point of view our proposed structure can be fabricated by standard extrusion and stacking methods. For fabrication purposes it is also very important to investigate the tolerance of the proposed structure with respect to the various design parameters. After investigating the effect of small variations in the values of d_1, d_2 and Λ we have found that the magnitude of dispersion and the effective mode area of propagating mode are less sensitive to the structural parameters. As shown in Fig. 7(a

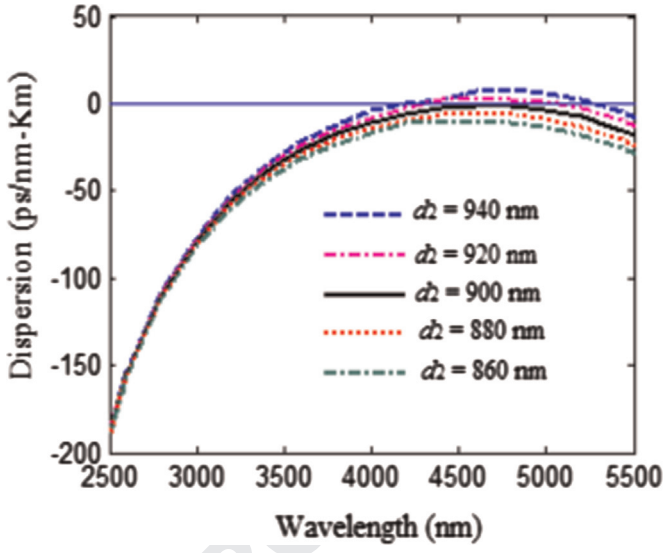

Fig. 4. Influence of hole diameter (d_2) on the dispersion characteristics of proposed structure while keeping other parameters fixed (i.e. Λ=1.2 μm and d_1=430 nm).

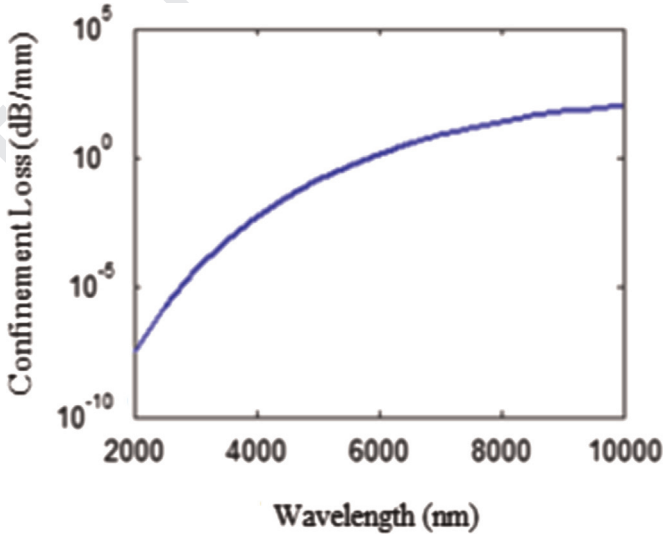

Fig. 5. The confinement loss of propagating mode of proposed TC PCF when Λ=1.2 μm, d_1=430 nm and d_2=900 nm.

Table 1
Geometrical parameters of proposed PCF.

Parameter name	Pitch	d_1	d_2
Parameter value	1.2 μm	430 nm	900 nm

and b), at 4.5 μm wavelength 1% deviations in d_1 changes the effective index value by ~0.03% and it also changes the effective mode area by ~0.56%. Similarly, 1% deviation in d_2 changes the effective index by ~0.01% and changes the effective mode area by 0.40% while, 1% deviation in Λ changes the effective index by 0.13% and changes the effective mode area by 2.31%.

4. Simulation of supercontinuum generation in proposed TC PCF

To simulate SCG in proposed PCF structure, we have to solve the generalized nonlinear Schrodinger Eq. (5) for pulse

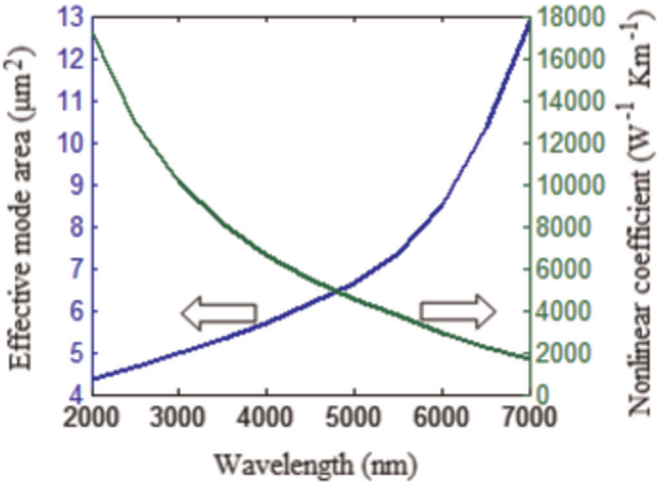

Fig. 6. The variation of effective mode area of propagating mode and corresponding nonlinear coefficient of proposed TC PCF with optimized parameters.

propagation in PCF structure. Eq. (5) represents GNLSE in time domain (TD). The drawback in implementation of this equation is that the time derivatives lead to numerical errors due to the discretization of the time window. When we write this equation in frequency domain, these derivatives vanish leaving only the discrete longitudinal step size as the source of numerical errors. In frequency domain Eq. (5) can be written as

$$\frac{\partial \tilde{A}}{\partial z} + \frac{\alpha}{2}\tilde{A} + i\tilde{A}\left(\beta(\Omega) - \beta_0 - \beta_1\Omega\right) = i\gamma\left(1 + \frac{\Omega}{\omega_0}\right) \times \left(F\left[\left(1 - f_R\right)A|A|^2 + f_R A F^{-1}[\tilde{h}_R F[|A|^2]]\right]\right) \quad (10)$$

where $\tilde{A}(z,\ \Omega)$ is the Fourier transform of $A(z,\ t)$, $\Omega = \omega - \omega_0$, F and F^{-1} stands for Fourier transform and inverse Fourier transform respectively, and $\tilde{h}_R = F(h_R(t))$. In above expression the arguments of both $\tilde{A}(z,\ \Omega)$ and $A(z,\ t)$ have been dropped. F and F^{-1} can be calculated numerically using the fast Fourier transform (FFT) and inverse fast Fourier transform (IFFT) respectively. For simulating SCG in proposed PCF structure we have solved Eq. (10) using interaction picture method in combination with conservation quantity error adaptive step-size algorithm [48].

In order to get flat, smooth and broad supercontinuum spectra we have selected pump wavelength at 4.5 μm in normal dispersion

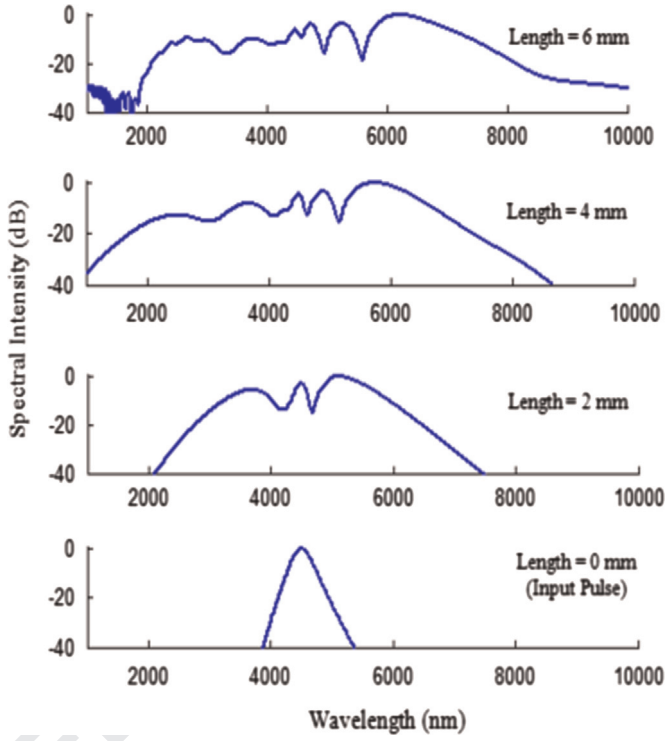

Fig. 8. Broadening of output spectra obtained at various lengths of TC PCF when peak power of incident pulse = 700 W and pulse duration (T_{FWHM}) = 50 fs.

regime with very small dispersion value of -2 ps/nm × Km for the proposed TC PCF. In our simulation, the peak power of incident pulse is 700 W with full-width at half maximum of 50 fs.

The calculated output spectra with different propagating length of PCF have been shown in Fig. 8. It has been observed that the spectral bandwidth starts to be broadened in only a few millimeter of propagation length. This feature of structure can be interpreted by comparing the nonlinear and dispersion length. The calculated values of nonlinear length ($L_{NL} = 1/\gamma P_0$) and dispersion length ($L_D = t_0^2/\beta_2$) for proposed TC PCF are 2.62×10^{-4} m and 6.49×10^{-2} m respectively at 4.5 μm pump wavelength. Since the nonlinear effect is stronger than dispersion effect, many of the new spectral components would be generated in a short length. After that the spectrum gets broadened due to the group velocity

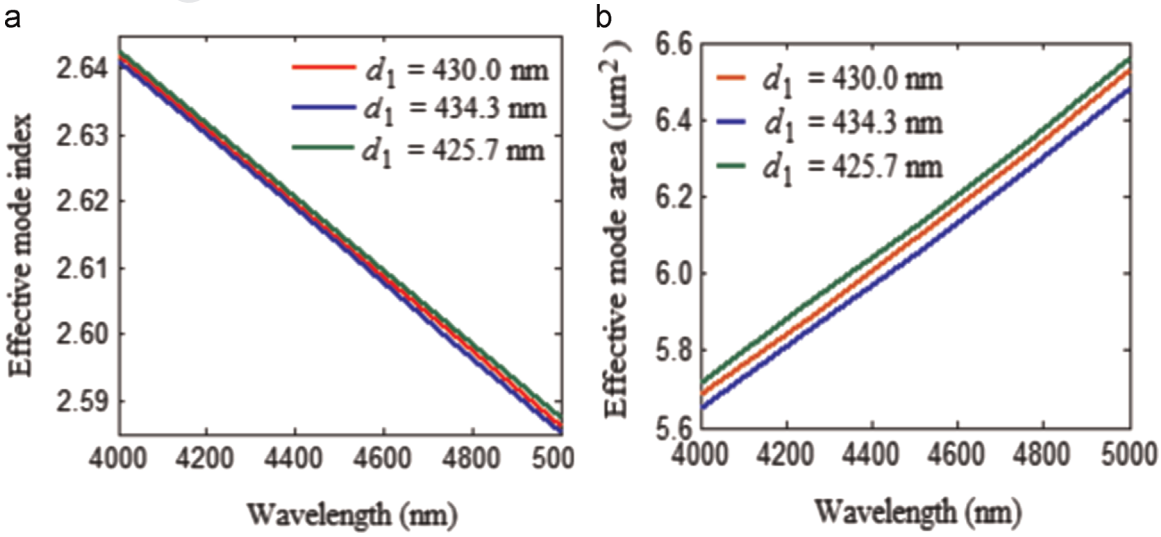

Fig. 7. Tolerance study of d_1: The effect on the effective mode index with ±1% deviation in d_1 (*a*); the effect on the effective mode area with ±1% deviation in d_1 (*b*).

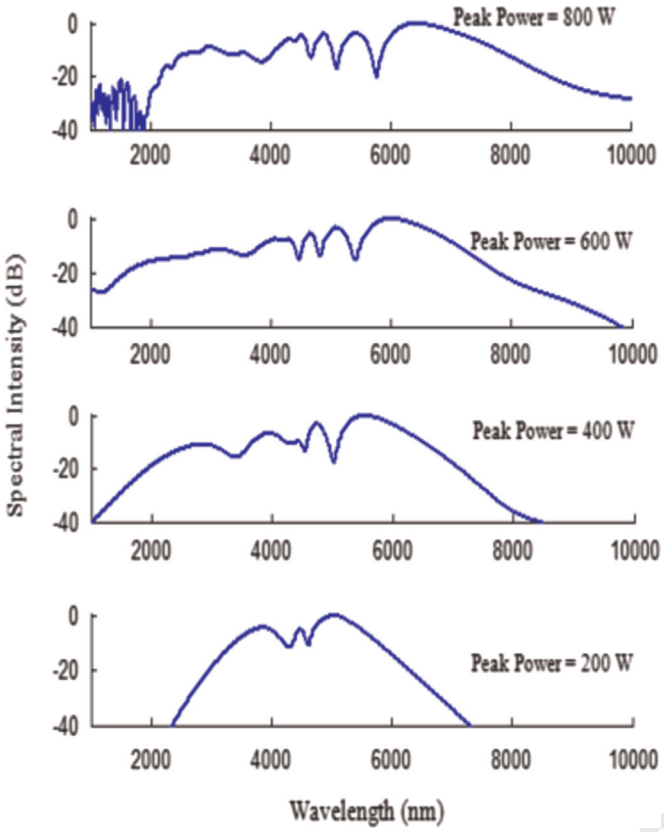

Fig. 9. Influence of input peak power on the broadening of output spectra with 50 fs incident pulse in 6 mm length of TC PCF.

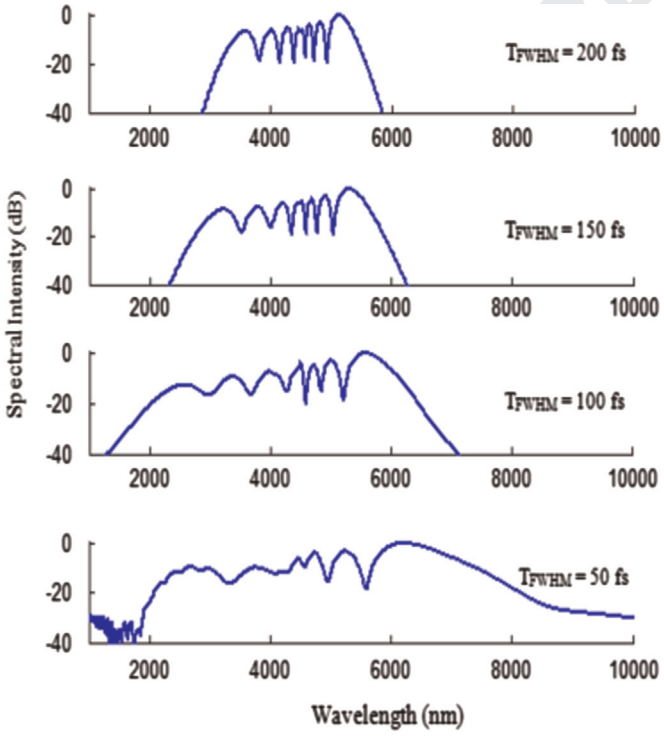

Fig. 10. Influence of full-width at half maximum (T_{FWHM}) of input pulse on the broadening of output spectra with 700 W peak power in 6 mm length of PCF.

dispersion (GVD) effect. It is to be noted that the output spectrum becomes constant in the 1.9–10 μm spectral range at the PCF length of 6 mm. In the initial phase of pulse propagation, SPM is responsible for symmetrical spectral broadening. As the PCF length is further extended, the Raman effect comes into account and extends the SC. Within 6 mm length of PCF an ultra-broadband SC extending from 1.9 μm to 10 μm at −30 dB level has been generated with 700 W peak power and 50 fs duration of input pulse. We have taken the power level −30 dB to compare our results with Ref. [45]. With further propagation the SC spectra does not change anymore.

Table 2
Optimized input pulse parameters.

Parameter name	Peak power	T_{FWHM}	Pulse shape
Parameter value	700 W	50 fs	hyperbolic secant

Fig. 9 illustrates the influence of input peak power on the bandwidth of output spectral intensity in 6 mm long PCF. The full-width at half maximum of the input pulse is fixed at 50 fs. Initially, the output spectra get broadened as the peak power of incident pulse increases. At high peak power, SPM effect dominants over dispersion effect. It has been observed that the maximum broadening in SC spectra is achieved at 700 W. Beyond this, no significant change in broadening has been observed, however, the flatness of SC spectra increases with further increase in peak power.

Finally, the influence of T_{FWHM} on the bandwidth of output spectral intensity in 6 mm long PCF has been shown in Fig. 10. The input peak power is fixed at 700 W. It is clear from figure that output spectra become narrow with increase in T_{FWHM}. This is due to SPM effect. It is to be noted that the short pulse is better to get broader SC spectra. The optimized values of input pulse are summarized in Table 2. It is to be mentioned that the coherence is also an important property of the SC spectra. However, in this paper, our focus is on the broad bandwidth of SC spectra using low pump power in a very small length of proposed TC PCF. Flatness and the coherence property is the subject of further investigation.

5. Conclusions

A new design of triangular core photonic crystal fiber with all-normal dispersion in As_2Se_3-based chalcogenide glass has been presented for ultra-broadband SCG. A flat-top dispersion curve with dispersion value approximately −2 ps/(nm × Km) in spectral range from 4.4 μm to 4.8 μm has been achieved. Proposed structure offers nonlinear coefficient as high as 5449 W^{-1} Km^{-1} at pump wavelength (i.e. 4.5 μm) with effective mode area of 6.15 μm^2. The influences of PCF length, input pulse peak power and full-width at half maximum (T_{FWHM}) on output spectral intensity have been investigated. Ultra-broadband SC spectra have been generated in a very small length of PCF with relatively low peak power of incident pulse. Simulated results indicate that the ultra-broadband SC extending from 1.9 μm to 10 μm at the −30 dB level can be generated in only 6 mm long As_2Se_3-based chalcogenide PCF with an input pulse peak power of 700 W in femtosecond regime. This new type of photonic crystal fiber can be a good candidate for generating efficient supercontinuum which is applicable for various nonlinear applications such as optical coherence tomography, pump-probe spectroscopy, metrology, nonlinear microscopy and frequency combs generation. Further, it is expected that the broadband range of the supercontinuum can be tuned and enhanced with new design of PCF.

Acknowledgments

The authors gratefully acknowledge the (*i*) initiatives and support towards establishment of the "TIFAC-Center of Relevance and Excellence" in Fiber Optics and Optical Communication at Delhi Technological University (Formerly Delhi College of Engineering) Delhi, through the "Mission REACH" program of Technology Vision-2020 of the Government of India and (*ii*). TUN-IND bilateral research project "Design, modeling and characterization of highly nonlinear fibers for all-optical high bit-rate network," funded by Ministry of Higher Education and Scientific Research of Republic of Tunisia and Department of Science and Technology, Govt. of India.

References

[1] G.P. Agrawal, Nonlinear Fiber Optics, 5th ed., Elsevier Academic Press, 2013.
[2] P. Russell, Photonic crystal fibers, Science 299 (2003) 358–362.
[3] J.M. Dudley, G. Genty, S. Coen, Supercontinuum generation in photonic crystal fiber, Rev. Mod. Phys. 78 (2006) 1135–1184.
[4] R.K. Sinha, S.K. Varshney, Dispersion properties in photonic crystal fibers, Microw. Opt. Tech. Lett. 37 (2003) 129–132.
[5] B. Dabas, R.K. Sinha, Dispersion characteristics of hexagonal and square lattice chalcogenide As_2Se_3 glass photonic crystal fiber, Opt. Commun. 283 (2010) 1331–1337.
[6] B. Dabas, R.K. Sinha, Design of highly birefringent chalcogenide glass PCF: a simplest design, Opt. Commun. 284 (2011) 1186–1191.
[7] T.S. Saini, A. Kumar, R.K. Sinha, Triangular-core large-mode-area photonic crystal fiber with low bending loss for high power applications, Appl. Opt. 53 (2014) 7246–7251.
[8] H. Ademgil, S. Haxha, Highly nonlinear birefringent photonic crystal fiber, Opt. Commun. 282 (2009) 2831–2835.
[9] S. Haxha, H. Ademgil, Novel design of photonic crystal fibers with low confinement losses, nearly zero ultraflatted chromatic dispersion, negative chromatic dispersion and improved effective mode area, Opt. Commun. 281 (2010) 278–286.
[10] S. Ghosh, R.K. Varshney, B.P. Pal, Generation of a low divergent supercontinuum for mid-IR high power delivery through a large mode area photonic bandgap fiber, Laser Phys. 23 (2013) 095105.
[11] D.J. Jones, S.A. Diddams, J.K. Ranka, A. Stentz, R.S. Windeler, J.L. Hall, S. T. Cundiff, Carrier-envelope phase control of femtosecond mode-locked lasers and direct optical frequency synthesis, Science 288 (2000) 635–639.
[12] B. Povazay, K. Bizheva, A. Unterhuber, B. Hermann, H. Sattmann, A.F. Fercher, W. Drexler, A. Apolonski, W.J. Wadsworth, J.C. Knight, P.S. Russell, M. Vetterlein, E. Scherzer, Submicrometer axial resolution optical coherence tomography, Opt. Lett. 27 (2002) 1800–1802.
[13] H.N. PaulseN, K.M. Hilligse, J. Thogersen, S.R. Keiding, J.J. Larsen, Coherent anti-Stokes Raman scattering microscopy with a photonic crystal fiber based light source, Opt. Lett. 28 (2003) 1123–1125.
[14] S. Sanders, Wavelength-agile fiber laser using group-velocity dispersion of pulsed super-continua and application to broadband absorption spectroscopy, Appl. Phys. B: Laser and Opt. 75 (2002) 799–802.
[15] S. Dupont, C. Petersen, J. Thogersen, C. Agger, O. Bang, S.R. Keiding, IR microscopy utilizing intense supercontinuum light source, Opt. Express 20 (2012) 4887–4892.
[16] A. Schliesser, N. Picque, T.W. Hansch, Mid-infrared frequency combs, Nat. Photon 6 (2012) 440–449.
[17] T. Morioka, K. Mori, S. Kawanishi, M. Saruwatari, Multi-WDM-channel GBit/s pulse generation from a single laser source utilizing LD-pumped supercontinuum in optical fibers, IEEE Photon, Technol. Lett 6 (1994) 365–368.
[18] R.R. Alfano, S.L. Shapiro, Emission in the region 4000 to 7000 < FigureObject > via four-photon coupling in glass, Phys. Rev. Lett. 24 (1970) 584.
[19] J.K. Ranka, R.S. Windeler, A.J. Stentz, Visible continuum generation in air silica microstructured optical fibers with anomalous dispersion at 800 nm, Opt. Lett. 25 (2000) 25–27.
[20] G. Genty, S. Coen, J.M. Dudley, Fiber supercontinuum sources, J. Opt. Soc. Am. B 24 (2007) 1771–1785.
[21] J.M. Dudley, J.R. Taylor, Supercontinuum Generation in Optical Fibers, Cambridge University Press, 2010.
[22] A. Barh, S. Ghosh, G.P. Agrawal, R.K. Varshney, I.D. Aggarwal, B.P. Pal, Design of an efficient mid-IR light source using chalcogenide holey fibers: a numerical study, J. Opt. 15 (2013) 035205.
[23] M. El-Amraoui, G. Gadret, J.C. Jules, J. Fatome, C. Fortier, J. Troles, Microstructured chalcogenide optical fibers from As_2S_3 glass: towards new IR broadband sources, Opt. Express 18 (2010) 26655–26665.
[24] L. Liu, G. Qin, Q. Tian, D. Zhao, W. Qin, Numerical investigation of mid-infrared supercontinuum generation up to 5 μm in single mode fluoride fiber, Opt. Express 19 (2011) 10041–10048.
[25] V. Shiryaev, M. Churbanov, Trends and prospects for development of chalcogenide fibers for mid-infrared transmission, J. Non-Cryst. Solids 377 (2013) 225–230.
[26] R.E. Slusher, G. Lenz, J. Hodelin, J. Sanghera, L.B. Shaw, I.D. Aggarwal, Large Raman gain and nonlinear phase shift in high-purity As_2Se_3 chalcogenide fibers, J. Opt. Soc. Am. B 21 (2004) 1146–1155.
[27] L.B. Shaw, V.Q. Nguyen, J.S. Sanghera, I.D. Aggarwal, P.A. Thielen, and F.H. Kung, IR supercontinuum generation in As–Se photonic crystal fiber, in: Proceedings of Advanced Solid State Photonics, paper TuC5, 2005.
[28] D.-I. Yeom, E.C. Magi, M.R.E. Lamont, M.A.F. Roelens, L. Fu, B.J. Eggleton, Low-threshold supercontinuum generation in highly nonlinear chalcogenide nanowires, Opt. Lett. 33 (7) (2008) 660–662.
[29] D.D. Hudson, S.A. Dekker, E.C. Magi, A.C. Judge, S.D. Jackson, E. Li, J.S. Sanghera, L.B. Shaw, I.D. Aggarwal, B.J. Eggleton, Octave spanning supercontinuum in an As_2S_3taper using ultralow pump pulse energy, Opt. Lett. 36 (7) (2011) 1122–1124.
[30] D.D. Hudson, E.C. Magi, A.C. Judge, S.A. Dekker, B.J. Eggleton, Highly nonlinear chalcogenide glass micro/nanofiber devices: design, theory, and octave-panning spectral generation, Opt. Commun. 285 (23) (2012) 4660–4669.
[31] M.R. Lamont, B. Luther-Davies, D. Choi, S. Madden, B.J. Eggleton, Supercontinuum generation in dispersion engineered highly nonlinear (γ=10/W/m) As_2S_3 chalcogenide planar waveguide, Opt. Express. 16 (19) (2008) 14938–14944.
[32] J. Hu, C.R. Menyuk, L.B. Shaw, J.S. Sanghera, I.D. Aggarwal, Maximizing the bandwidth of supercontinuum generation in As_2Se_3 chalcogenide fibers, Opt. Express 18 (2010) 6722–6739.
[33] C. Agger, C. Petersen, S. Dupont, H. Steffensen, J.K. Lyngso, C.L. Thomsen, J. Thogersen, S.R. Keiding, O. Bang, Supercontinuum generation in ZBLAN fibers – detailed comparison between measurement and simulation, J. Opt. Soc. Am. B 29 (2012) 635–645.
[34] I. Kubat, C.S. Agger, P.M. Moselund, O. Bang, Mid-infrared supercontinuum generation to 4.5 μm in uniform and tapered ZBLAN step-index fibers by direct pumping at 1064 or 1550 nm, J. Opt. Soc. Am. B 30 (2013) 2743–2757.
[35] I. Kubat, C.R. Petersen, U.V. Moller, A. Seddon, T. Benson, L. Brilland, D. Mechin, P.M. Moselund, O. Bang, Thulium pumped mid-infrared 0.9–9 μm supercontinuum generation in concatenated fluoride and chalcogenide glass fibers, Opt. Express 22 (2014) 3959–3969.
[36] D.D. Hudson, M. Baudisch, D. Werdehausen, B.J. Eggleton, J. Biegert, 1.9 octave supercontinuum generation in a As_2S_3 step-index fiber driven by mid-IR OPCPA, Opt. Lett. 39 (19) (2014) 5752–5755.
[37] I. Kubat, C.S. Agger, U. Moller, A.B. Seddon, Z. Tang, S. Sujecki, T.M. Benson, D. Furniss, S. Lamrini, K. Scholle, P. Fuhrberg, B. Napier, M. Farries, J. Ward, P. M. Moselund, O. Bang, Mid-infrared supercontinuum generation to 12.5μm in large NA chalcogenide step-index fibres pumped at 4.5 μm, Opt. Express 22 (2014) 19169–19182.
[38] Y. Takushima, F. Futami, K. Kikuchi, Generation of over 140-nm-wide supercontinuum from a normal dispersion fiber by using a mode-locked semiconductor-laser source, IEEE Photon, Technol. Lett 10 (1998) 1560–1562.
[39] A. Hartung, M. Heidt, H. Bartelt, Design of all-normal dispersion microstructured optical fibers for pulse-preserving supercontinuum generation, Opt. Express 19 (2011) 7742–7749.
[40] A.M. Heidt, Pulse preserving flat-top supercontinuum generation in all-normal dispersion photonic crystal fibers, J. Opt. Soc. Am. B 27 (2010) 550–559.
[41] A. Baili, R. Cherif, M. Zghal, New design of As2Se3-based chalcogenide photonic crystal fiber for ultra-broadband, coherent, mid-IR supercontinuum generation, Proc. SPIE, 8564–856409Proc. SPIE, 8564–856409.
[42] P. Yan, R. Dong, G. Zhang, H. Li, S. Ruan, H. Wei, J. Luo, Numerical simulation on the coherent time-critical 2–5 μm supercontinuum generation in an As_2S_3 microstructured optical fiber with all-normal flat-top dispersion profile, Opt. Commun. 293 (2013) 133–138.
[43] A. Baili, R. Cherif, A. Heidt, M. Zghal, Maximizing the bandwidth of coherent, mid-IR supercontinuum using highly nonlinear aperiodic nanofibers, J. Modern Optics 61 (2014) 650–661.
[44] M. Klimczak, B. Siwicki, P. Skibinski, D. Pysz, R. Stepien, A. Heidt, C. Radzewicz, R. Buczynski, Coherent supercontinuum generation up to 2.3 μm in all-normal soft-glass photonic crystal fibers with flat all-normal dispersion, Opt. Express 22 (2014) 18824–18832.
[45] W. Yuan, 2–10 μm mid-infrared supercontinuum generation in As_2Se_3 photonic crystal fiber, Laser Phys. Lett. 10 (2013) 095107.
[46] L. Sojka, Z. Tang, D. Furniss, H. Sakr, A. Oladeji, E. Beres-Pawlik, H. Dantanarayana, E. Faber, A.B. Seddon, T.M. Benson, S. Sujecki, Broadband, mid-infrared emission from Pr^{3+} doped GeAsGaSe chalcogenide fiber optically clad, Opt. Mater. 36 (2014) 1076–1082.
[47] B. Ung, M. Skorobogatiy, Chalcogenide microporous fibers for linear and nonlinear applications in the mid-infrared, Opt. Exp. 18 (2010) 8647–8659.
[48] A.A. Rieznik, A.M. Heidt, P.G. Konig, V.A. Bettachini, D.F. Grosz, Optimum integration procedures for supercontinuum simulation, J. IEEE Photon. 4 (2012) 552–560.

Please cite this article as: T. Singh Saini, et al., Optics Communications (2015), http://dx.doi.org/10.1016/j.optcom.2015.02.049